Journal of the Serbian Chemical Society
JSCS-info@shd.org.rs • www.shd.org.rs/JSCS
J. Serb. Chem. Soc. *87* (4) 479–490 (2022)
JSCS–5535
Original scientific paper
Published 18 February 2022

Rate coefficients for electron-impact dissociation of O_3^+ to singly charged fragments

DRAGOLJUB S. BELIĆ[1], MIRJANA M. VOJNOVIĆ[1], MIROSLAV M. RISTIĆ[2*#], XAVIER URBAIN[3] and PIERRE DEFRANCE[3]

[1]*University of Belgrade, Faculty of Physics, P. O. Box 44, 11000 Belgrade, Serbia,* [2]*University of Belgrade, Faculty of Physical Chemistry, P. O. Box 47, 11000 Belgrade, Serbia and* [3]*Université Catholique de Louvain, Institute of Condensed Matter and Nanosciences, Chemin du Cyclotron 2, B-1348 Louvain-la-Neuve, Belgium*

(Received 9 November, revised 11 December, accepted 13 December 2021)

Abstract: Rate coefficients for electron-impact dissociation of O_3^+ to the O^+ and O_2^+ fragments are calculated for the new, recommended cross section data set and for various collisional conditions. Two sets of the cross section data, measured recently by different experimental groups, are used. These cross sections differ significantly with each other, but are renormalized and optimized to the coherent data base. Rate coefficients for the ozone cation fragmentation are determined using the Maxwellian and the non-thermal electron energy distribution functions (EEDF). In the case of Maxwellian distribution, mean electron energies cover the range from zero up to 2 keV. Non-thermal electron energy distribution functions are adopted from the recent electron observations by the 3-D plasma and energetic particles experiment on the WIND spacecraft. The non-thermal rates are evaluated for the mean electron energies from 4 to 80 eV. The role of the possible contribution of electron-impact dissociation of O_3^+ to the ozone layer depletion has been emphasized.

Keywords: ozone cation; electron-molecule collisions; dissociative ionization, dissociative excitation.

INTRODUCTION

The problem of ozone layer depletion in the stratosphere is attracting significant attention of researchers, after the discovery of the Antarctic ozone hole.[1,2] Various mechanisms contributing to the ozone molecule decomposition have been investigated in the past decades. A significant influence is attributed to the air pollutants, such as nitric oxides, as well as chlorine and bromine compounds.[3] It has been recognized that the absorption of UV light leads to the ozone layer

* Corresponding author. E-mail: ristic@ffh.bg.ac.rs
# Serbian Chemical Society member.
https://doi.org/10.2298/JSC211109110B

depletion, but some molecular reactions and collisions with atoms, ions and electrons present in the stratosphere are also found to play a role.[4–6]

Electron-impact ionization of ozone has been studied experimentally,[7,8] and also theoretically.[9] These data are renormalized by the NIST Standard Reference Database.[10] The renormalized cross section magnitude amounts $(3.8\pm0.5)\times10^{-16}$ cm^2, at the maximum at 100 eV, with the threshold energy of 13.2±0.5 eV. Visible and ultra violet (VUV) optical absorption and electron energy-loss spectroscopy of ozone have also been investigated and reviewed in detail.[11]

The ozone cation O_3^+ exists naturally in the atmosphere and is important for our understanding of ozone depletion as well.[12] The theoretical calculation of the electronic structure of the ozone cation is complex due to the strong electron correlations and a significant lacking of details of its potential energy surfaces. O_3^+ is nonlinear and the bond distances and angles differ significantly for each electronic state. The three lowest doublet states are assigned X^2A_1, A^2B_2, and B^2A_2 and their energies are all within 1 eV apart. The calculations show that the three lower quartet states are also close in energy, lying up to 2 eV above the ground state. The ozone cation is weakly bound and easily dissociates by photon absorption, electron collision, or recombination.

Electron-impact dissociative recombination of O_3^+ has been investigated by the ion storage-ring method.[13] This collision process is dominated at 0 eV by the three-body dissociation. The photo-dissociation of O_3^+ yielding O^+ or O_2^+ fragments has also been studied intensively. It has been concluded that the formation of the O^+ prevails in the visible light range.[14]

Electron-impact dissociation of O_3^+ has recently been investigated in two separate experiments.[15,16] The charged fragments, O^+ and O_2^+ were mass analyzed and the cross sections for their production were determined in a wide electron energy range.

In the present study, the above cited experimental results of O_3^+ fragmentation are revisited. Some of the results are renormalized and the cross-section database is completed. In addition, the rate coefficients for corresponding processes, for Maxwellian and non-thermal electron energy distribution functions, are calculated and compared with each other. The following reactions are considered here:

$$e^- + O_3^+ \rightarrow O^+ + O_2 + e^- \quad (0.64\ eV) \qquad (1)$$

$$e^- + O_3^+ \rightarrow O_2^+ + O + e^- \quad (2.19\ eV) \qquad (2)$$

$$e^- + O_3^+ \rightarrow O^+ + O_2^+ + 2e^- \quad (14.26\ eV) \qquad (3)$$

The energies written in the parentheses represent the threshold energies for the given processes.[15] Reactions (1) and (2) are dissociative excitation (DE) processes, while reaction (3) represents dissociative ionization (DI).[16] In both exp-

eriments, only the charged fragments are detected, independently from each other. The reactions involving dissociation to three particles are not considered here.

Absolute cross sections for electron-impact dissociation of O_3^+ to the O^+ and to O_2^+ fragments have been measured first at ORNL, by Deng *et al.*[15] An electron-ion crossed-beam method has been used for energies from about 3 to 100 eV. While the O_2^+ channel dominates the dissociation cross section over the entire electron energy range, a strong rise is also observed in the O^+ product channel, just above the threshold energy.

The cross sections for dissociation of O_3^+ to the O^+ fragments were also measured recently, at UCL (Louvain-la-Neuve), by Belić *et al.*[16] This experiment also used a crossed-beam technique, but the results for dissociation producing the O^+ fragments disagree for a factor between 2 and 3, in a wide electron energy range, above 5 eV, the UCL results being larger than those of ORNL. This has been attributed to the broad O^+ fragments velocity and scattering angle distributions in the laboratory frame, causing a possible loss of the signal in the ORNL experiment. This effect is strongly affecting the DI signal leading to O^+. It has been corrected in UCL experiment by performing careful magnetic field scans of the signal and by taking into account the transmission efficiency of the experiment. The correction procedure has been described in detail.[16]

The maximum of the O^+ cross section is found to be 3.6×10^{-16} cm^2 at about 100 eV and has an average value of 3×10^{-16} cm^2 in a wide energy range from 5 to 200 eV.[16] Such a broad energy interval of high cross sections may result in a higher rate coefficient values for the considered process. Thus, we can raise the question of the importance of electron-impact dissociation of the ozone cation in the stratospheric layer, relative to the other competitive mechanisms. Furthermore, it may be possible that the electrons, originating from the Solar wind and penetrating in the stratosphere along the polar cusps, play an important role in the Ozone layer depletion. This possibility initiated this work and will be considered later in the text.

EXPERIMENTAL

Cross sections database

The cross sections, used here for the rate coefficient calculations, were measured by Deng and coworkers,[15] and later by Belić *et al.*[16] These are the only experimental results for electron-impact fragmentation of O_3^+. In the ORNL experiment,[15] both cross sections, for O^+ and O_2^+ fragments were measured.

In the UCL experiment,[16] the cross sections are reported for the O^+ fragment production, only. An attempt to measure cross sections for the O_2^+ fragments failed, because enormous background count rate was present for this particular ion.

In the cited experiments, electron-impact simple ionization cross section of O_3^+ resulting in O_3^{2+} was found to be negligible. This finding is in agreement with the conclusion of Deng *et al.*[15] We believe that the lifetime of the doubly charged ozone ion O_3^{2+} is shorter than the time scale of the experiments and that it dissociates before reaching the detector.

As in many other electron-ion dissociation experiments in the UCL laboratory, particular attention has been paid to the total detection of the product ions (see for example the proposed references).[17-19] Due to the transfer of internal energy to the kinetic energy of the fragments, dissociation products exhibit both broad velocity distribution and a broad angular divergence in the laboratory frame. This often results in a partial loss of the signal. In order to compensate for this effect, careful analyzer magnetic-field scans of the signal have been performed for the selected electron energies (see for instance Fig. 1 in a publication by Belić *et al.*[16]). These scans are used: *i*) to normalize measurements to the absolute scale, *ii*) to determine total kinetic energy release (KER) distribution of the fragments, which illustrates Fig. 4 in a paper by Belić and coworkers,[16] and consequently *iii*) to separate DE and DI contributions of the inclusive cross sections. In the present work, magnetic-field scans will be further used to estimate a new set of the cross section data for the O_2^+ fragment production *i.e.* to renormalize previous measurements of ORNL group. This is performed by taking into account proper transmission efficiency of the experiment, determined for the O^+ fragment and by applying it to the O_2^+ fragment. Our goal was to calculate and to compare resulting rate coefficients for O_3^+ fragmentation by electron impact, for various reaction channels.

Renormalization of the O_2^+ cross-sections

We have learned (in earlier study)[16] that the difference between cross sections for O^+ fragment production in references[15,16] results mainly from the loss of the DI contribution in ORNL experiment.[15] Thus, similar effect can be expected for the O_2^+ fragments, as well. Furthermore, we have determined the DI cross section contribution for O^+ fragment[16] to be dominant over DE for energies above 40 eV (see Fig. 3 in Belić *et al.*[16]). Consequently, the UCL group found the inclusive cross section for this fragment to be significantly higher in a wide energy range, compared to the results of ORLN group. Since the DI reaction (3) is dominant channel for the creation of both O_2^+ and O^+ fragments, we could expect similar situation for O_2^+ fragments. For that reason, we have made an attempt to renormalize the ORNL cross section results for the O_2^+ fragments production.

For this purpose, magnetic-field scans obtained for the O^+ fragments, *i.e.*, the total KER distributions of product fragments (see Fig. 4 in a UCL reference)[16] are used. By applying Lorentz expression, these scans are first transformed to the center-of-mass velocity distribution of the O^+ fragments.[17] Under the assumption of dominant DI contribution and based on the momentum conservation, initial velocity distributions of the O_2^+ fragments, in the center-of-mass frame, are determined. The results are further transformed to the fragment distributions in the laboratory frame. Because of the larger mass, they have lower velocity than O^+ fragments, but are occurring at the larger analyzer magnetic fields. These distributions are used for Monte Carlo simulation of the expected magnetic-field scans of the fragments, according to the procedure described before.[18,19] Having these scans, the transmission efficiency for the O_2^+ fragments is determined to be between 30 and 42 %. The transmission factors are extrapolated to the considered electron energy range and are applied to the experimental cross sections published by Deng *et al.* for the O_2^+ fragments.[15]

In this way absolute cross sections for electron impact dissociation of O_3^+ producing the O_2^+ fragment, corrected for the experimental transmission and detection efficiency, are determined. They are shown in Fig. 1, together with the absolute cross sections for dissociation to the O^+ fragment.[16] The O_2^+ cross sections are also presented in Table I and will be referred hereafter as recommended cross sections. The total charged fragments production cross section, also shown in Fig. 1, is the sum of these two, O^+ and O_2^+ cross sections.

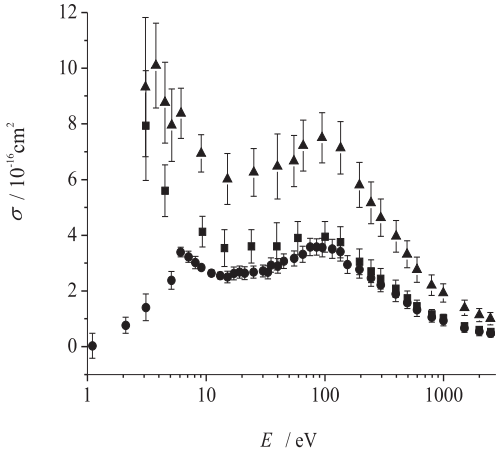

Fig. 1. Absolute cross sections for electron-impact dissociation of O_3^+ to O^+ (circles), O_2^+ (squares), and for total inclusive singly charged fragments production (triangles).

TABLE I. Recommended cross sections σ_r for electron-impact dissociation of O_3^+ yielding O_2^+ fragments, at various electron energies E

E / eV	σ_r / 10^{-16} cm^2	$\Delta\sigma_r$ / 10^{-16} cm^2	E / eV	σ_r / 10^{-16} cm^2	$\Delta\sigma_r$ / 10^{-16} cm^2
3.1	7.94	1.97	245.1	2.71	0.41
4.5	5.60	0.93	295.1	2.44	0.37
9.3	4.13	0.55	395.1	2.08	0.31
14.3	3.54	0.66	495.1	1.74	0.26
24.0	3.60	0.60	595.1	1.45	0.22
39.3	3.60	0.85	795.1	1.16	0.17
59.0	3.90	0.60	995.1	1.02	0.15
100.0	3.95	0.55	1495.1	0.73	0.11
135.1	3.75	0.56	1995.1	0.60	0.09
195.1	3.05	0.46	2495.1	0.53	0.08

Method of rate coefficient calculation

Rate coefficients have been calculated by using standard procedure,[20] given by the following expression:

$$K(\langle E\rangle) = \sqrt{\frac{2}{m}} \int_{E_{th}}^{\infty} \sigma(E)\sqrt{E} f_e(\langle E\rangle, E)\mathrm{d}E \tag{4}$$

where $\langle E\rangle$ is the mean electron energy, $\sigma(E)$ is the cross section for considered process, E_{th} is the threshold energy and $f_e(\langle E\rangle,E)$ is the normalized electron energy distribution function (EEDF). Calculations have been performed by using numerical interpolation of experimental cross section data. In case of equilibrium conditions, the EEDF in (4) is given by the Maxwellian equation:

$$f_e(\langle E\rangle, E) = \frac{2}{\sqrt{\pi}}\left(\frac{3}{2\langle E\rangle}\right)^{3/2} \sqrt{E}\mathrm{e}^{-3E/2\langle E\rangle} \tag{5}$$

For the non-Maxwellian, *i.e.*, non-equilibrium case, experimental EEDF-s for the mean electron energy values of 4.53, 6.4, 46.2 and 71.7 eV are used. They have been adopted from measurements of the non-thermal ”super-halo” component of the Solar wind electrons per-

formed with the help of 3-D Plasma and energetic particles experiment on the WIND spacecraft.[21] In the present study, two different EEDF functions at 71.7 eV are used, including WIND and "super-halo" projects, giving essentially the same rate coefficients.

The solar wind is a stream of charged particles (plasma) emitted from the upper atmosphere of the Sun. It consists predominantly of electrons and protons in the energy range up to 0.5 to 10 keV.

The solar wind varies in density, temperature and speed over time and distance. Its particles can escape the Sun's gravity because of their high energy resulting from the high temperature of the corona. The consequences of this are solar wind and geomagnetic storms on Earth, and the light auroras at the poles.

High energy cross sections and contributions of the related processes

Generally, normalized EEDF becomes lower, but wider with increasing the mean electron energy. In both cases, Maxwellian and non-equilibrium, rates are dependent on the cross section magnitude and its shape, *i.e.*, they are related to the cross section and EEDF overlap at a given mean electron energy. This will be illustrated here for the O^+ fragments. In UCL experiment,[16] DE and DI contributions for this fragment are separated (see Fig. 3 in the cited work).[16] The two cross sections are used to calculate Maxwellian rate coefficients for these particular processes. The results are compared in Fig. 2.

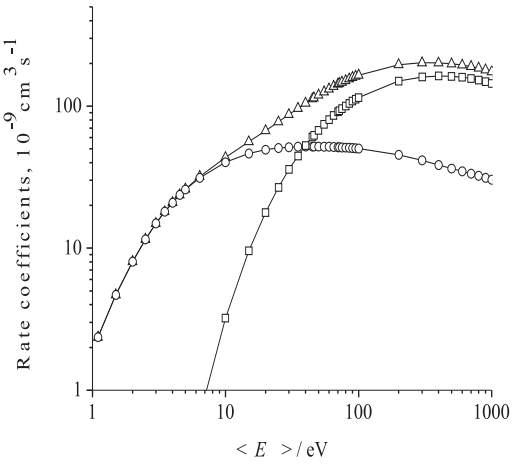

Fig. 2. Maxwellian rate coefficients for DE (circles), DI (squares) and inclusive cross-sections (triangles) for O^+ fragment production.

The DE cross sections are higher than those for DI at low mean electron energy, below 40 eV. However, it turned out that corresponding rates at higher mean electron energies are up to a factor of 5 larger for DI than those for DE, Fig. 2. The total rate coefficients for O^+ production reach 2×10^{-7} cm^3 s^{-1} in a wide mean electron energy range, above 100 eV.

The comparison of these data is also performed with the results of rate coefficients calculated with corresponding cross sections for O^+ fragments published by Deng *et al.*[15] These rates are a factor of 3 lower than the present total inclusive rates shown in Fig. 2.

Similar, or even more pronounced effects are expected for non-thermal EEDF-s. Enhancements may be expected for processes which include high energy reactions, such as inner shell or multiple ionization.

Moreover, it should be pointed out that the Energetic electron precipitation (EEP) plays even more prominent role and affects the chemical composition of the polar mesosphere.[22] It

leads to odd hydrogen (HO_x) production following ionization and ion chemical reactions, which are expected to contribute to the ozone balance in the mesosphere.

It has been shown,[23] using observations from three different satellite instruments, that EEP events strongly affect ozone at 60–80 km, leading to extremely large (up to 90 %) short--term ozone depletion. This impact is comparable to that of large, but much less frequent, solar proton events. On solar cycle timescales, it has been found that EEP causes ozone variations of up to 34 % at 70–80 km altitude. With such a magnitude, it is reasonable to suspect that EEP could be an important part of solar influence on the atmosphere and climate system.

RESULTS AND DISCUSSION

Maxwellian and non-thermal rate coefficients for electron impact dissociation of O_3^+ to the O^+ and O_2^+ fragments were calculated and are presented herein. The Maxwellian rates were determined in the mean electron energy range from 0 to 2 keV. The non-thermal rates were determined for the mean energies from 4 to 80 eV, for the experimental EEDF-s.[21] These calculations were performed for the present recommended cross section data set (for the O^+ fragment of reference[16] and for renormalized cross sections for the O_2^+ fragment, presented herein). Rate coefficients for the total singly charged fragments production, K_T, were obtained as the sum of these two results.

For comparison purposes, calculations are also performed using the cross sections for O^+ and O_2^+ measured directly and published by Deng *et al.*[15] Rate coefficients for the total singly charged fragments production, K_T, were also obtained in this case.

Maxwellian rate coefficients

The results for the Maxwellian rate coefficients were calculated using Eqs. (4) and (5). They are presented in Table II, and also shown in Fig. 3. The lowest curve in Fig. 3, shown by circle symbols was obtained by using the cross section measurements of Belić *et al.* for O^+.[16] These results are denoted $K(O^+)$ in Table II. The data represented by squares in Fig. 3 were obtained using the recommended cross section results for O_2^+, and they are marked $K(O_2^+)$ in Table II. The results denoted by K_T ($O^+ + O_2^+$) in Table II and by triangles in Fig. 3 represent the sum of these two results and are in fact the total inclusive rate for producing singly charged fragments by electron impact dissociation of O_3^+. As could be noticed, the $K(O_2^+)$ results are higher over the whole range of considered mean electron energy than those for the O^+ fragments. This is expected bearing in mind that the cross sections for O_2^+ are higher for all energies than those for O^+, particularly for the low energies near threshold, see Fig. 1.

The rates $K(O^+)$ and $K(O_2^+)$ have maximum values slightly above 2×10^{-7} $cm^3\ s^{-1}$, at about 300 eV. The total rate K_T ($O^+ + O_2^+$) has a maximum value of 4.27×10^{-7} $cm^3\ s^{-1}$ also at 300 eV. For the purpose of comparison, the ORNL cross-sections of Deng *et al.*,[15] were extrapolated to the high energy side and all rates were calculated for the mean electron energies up to 2 keV. These rates

were determined for the O^+ and O_2^+ fragments, respectively. However, they were lower than 10^{-7} cm^3 s^{-1} over the whole energy range and are not presented herein. The sum of these two contributions for this data set had a maximum of 1.6×10^{-7} cm^3 s^{-1} at about 250 eV and fell to a quarter of this value at 2 keV.

TABLE II. Maxwellian rate coefficients, K / 10^{-7} cm^{3}s^{-1}, for electron-impact dissociation of O_3^+ to O^+, O_2^+, and for the total inclusive production of singly charged fragments, K_T

E / eV	$K(O^+)$	$K(O_2^+)$	K_T	E / eV	$K(O^+)$	$K(O_2^+)$	K_T
1	0.02	0.052	0.062	200	1.95	2.17	4.12
2	0.08	0.23	0.28	250	2.00	2.22	4.21
3	0.15	0.37	0.52	300	2.01	2.23	4.27
4	0.21	0.46	0.68	350	2.02	2.23	4.25
5	0.26	0.53	0.79	400	2.04	2.22	4.23
6	0.30	0.57	0.89	450	2.00	2.21	4.21
7	0.34	0.62	0.97	500	1.98	2.20	4.17
8	0.37	0.65	1.04	550	1.96	2.17	4.14
9	0.40	0.68	1.09	600	1.94	2.15	4.09
10	0.43	0.71	1.15	650	1.92	2.12	4.05
20	0.67	0.92	1.59	700	1.90	2.10	3.99
30	0.87	1.11	1.98	750	1.88	2.08	3.95
40	1.02	1.27	2.32	800	1.85	2.04	3.89
50	1.21	1.43	2.60	850	1.83	2.02	3.94
60	1.33	1.54	2.83	900	1.80	1.98	3.78
70	1.42	1.63	3.04	950	1.77	1.95	3.73
80	1.51	1.72	3.22	1000	1.76	1.92	3.67
90	1.59	1.81	3.39	1500	1.48	1.63	3.09
100	1.66	1.85	3.50	2000	1.24	1.37	2.60
150	1.85	2.08	3.93				

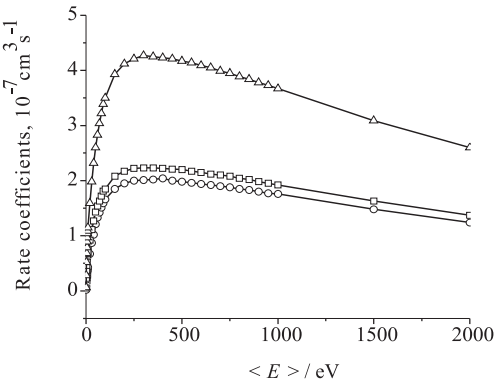

Fig. 3. Maxwellian rate coefficients for O_3^+ dissociation to O^+ (circles), O_2^+ (squares) and for the total inclusive production of singly charged fragments K_T (triangles). For explanation see the text.

The results for the present data set are more than a factor of two higher than the values obtained for the data set of Deng *et al.*,[15] for all energies. This has a simple explanation. The cross sections used herein for the present data set are corrected to the loss of signal and are higher than in ORNL experiment.[15] Of

particular interest is the fact that this lost signal originates mainly due to the DI contribution, which prevails in the higher incident electron energy range. Therefore, this results in a significant increase in the rate coefficients, relative to the previous data.[15]

Non-thermal rate coefficients

Non-Maxwellian (or non-thermal) rate coefficients are calculated for the same sets of cross section data, as above for the Maxwellian case. EEDF-s were available only for four mean electron energies in the range from 4.53 to 71.7 eV.[21] The non-thermal rates obtained upon using these EEDFs in Eq. (4) were interpolated and extrapolated across the energy range from 4 to 80 eV, in order to make comparison with the Maxwellian rate coefficients.

The non-thermal rates for the present data set are listed in Table III and are also shown in Fig. 4, along with the Maxwellian ones. In the considered energy range, non-thermal rates do not reach their maxima. Their highest values for $<E>$ = 80 eV is 2.0×10^{-7} cm^3 s^{-1} for $K(O^+)$, and 2.25×10^{-7} cm^3 s^{-1} for $K(O_2^+)$. Thus, the total inclusive rate amounts to 4.25×10^{-7} cm^3 s^{-1} at $<E>$ = 80 eV. This could be compared to the value of 3.22×10^{-7} cm^3 s^{-1} obtained for the Maxwellian total inclusive rate coefficient (for the same mean electron energy), which is lower byr some 25 %. Generally, the non-thermal rates are higher than the Maxwellian ones, for all reaction channels and for all electron energies.

TABLE III. Non-thermal rate coefficients, K / 10^{-7} cm^3 s^{-1}, for electron-impact dissociation of O_3^+ to O^+, O_2^+, and for the total inclusive production of singly charged fragments, K_T

E / eV	$K(O^+)$	$K(O_2^+)$	K_T	E / eV	$K(O^+)$	$K(O_2^+)$	K_T
4	0.38	0.67	1.07	25	1.10	1.32	2.40
5	0.43	0.71	1.15	30	1.24	1.45	2.70
6	0.46	0.74	1.22	35	1.36	1.56	2.91
7	0.50	0.78	1.29	40	1.48	1.67	3.14
8	0.54	0.81	1.36	45	1.59	1.78	3.35
9	0.58	0.84	1.42	50	1.68	1.87	3.55
10	0.61	0.87	1.49	55	1.76	1.96	3.70
12	0.68	0.94	1.62	60	1.83	2.03	3.87
14	0.75	1.00	1.75	65	1.88	2.09	3.96
16	0.82	1.06	1.88	70	1.94	2.15	4.08
18	0.88	1.12	2.00	75	1.99	2.20	4.17
20	0.94	1.18	2.12	80	2.00	2.24	4.25

For non-thermal EEDF-s, the results based on the ORNL cross-section measurements are lower than for the present set of data. The rate coefficient values are lower by even a factor of 2, for most of electron energies, and up to a factor of 3 for the high ones.

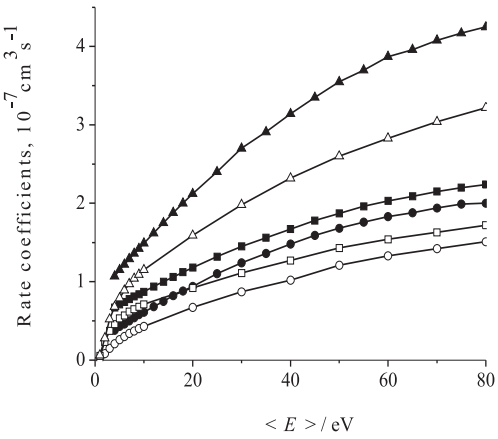

Fig. 4. Non-thermal rate coefficients (closed symbols) and Maxwellian rate coefficients (open symbols) for O_3^+ dissociation to O^+ (circles), O_2^+ (squares) and for the total inclusive singly charged fragments production K_T (triangles).

Comparison of Maxwellian and non-thermal rate coefficients

As already pointed out, due to the larger cross section values, the rate coefficients are higher for the present data set than for those based on the ORNL data. This was observed using both the Maxwellian and non-thermal EEDF-s. The reason for this is attributed to the loss of signals, *i.e.*, underestimated cross sections in the earlier data set, which were recuperated in the present data. This is clearly seen in particular for the high mean electron energies. Thus, the rate coefficient results based on the ORNL data will not be further considered herein and are not recommended for use in modeling the balance of ozone in the Earth's atmosphere.

Finally, we shall discuss the rate coefficient dependance on the used EEDF-s. For the purpose of comparison, we redirect reader's attention again to the Tables II and III. For all considered processes, the rate coefficients calculated by using available non-thermal EEDF-s are higher than for the case of Maxwellian EEDF. This is the consequence of the behavior of the cross sections. They have large values extended to relatively high electron energies, thus their overlapping integral with non-thermal EEDF-s is higher that with Maxwellian ones, in a wide energy range. Consequently, non-thermal rate coefficients are additionally magnified.

The effects of external electric or magnetic fields, or their combination, on the rate coefficients wereare not investigated in the present work. This obviously needs to be studied in detail, in future investigations.

CONCLUSIONS

Rate coefficients were calculated for electron-impact dissociation of O_3^+ to the O^+ and O_2^+ fragments. Experimental cross section results for O^+ fragments from Belić *et al.*[16] and renormalized data for O_2^+ fragment from Deng *et al.*[15] were used. Maxwellian and non-equilibrium EEDF-s were applied for the mean electron energies from threshold up to 2 keV. Significantly higher rate coefficients were observed for the present results than for those measured by the

ORNL group. Rate coefficients for non-equilibrium EEDFs were found to be higher by a factor of two than for the Maxwellian ones. Thus, the investigated processes were found likely to play an even more important role in the ozone cation dissociation, than had previously been expected.

This work demonstrates that the Solar wind electrons, penetrating in the Earth's stratosphere along the polar cusps, can make significant contribution in the Ozone layer depletion and should be included in future modeling.

Acknowledgements. This work was supported by the Fonds de la Recherche Scientifique – FNRS through IISN Contract No. 4.4504.10. The authors value the financial support of the Association Euratom-Belgian State. D.S.B. is grateful for support from Project No. 171016 from the Ministry of Education, Science and Technological Development of the Republic of Serbia.

ИЗВОД

КОЕФИЦИЈЕНТИ БРЗИНЕ ЗА ДИСОЦИЈАЦИЈУ O_3^+ УДАРОМ ЕЛЕКТРОНА НА ЈЕДНОСТРУКО НАЕЛЕКТРИСАНЕ ФРАГМЕНТЕ

ДРАГОЉУБ С. БЕЛИЋ[1], МИРЈАНА М. ВОЈНОВИЋ[1], МИРОСЛАВ М. РИСТИЋ[2], XAVIER URBAIN[3] и PIERRE DEFRANCE[3]

[1]Универзитет у Београду – Физички факултет, Студентски трг 16, Београд, [2]Универзитет у Београду – Факултет за физичку хемију, Студентски трг 12–16, Београд и [3]Université Catholique de Louvain, Institute of Condensed Matter and Nanosciences, Chemin du Cyclotron 2, B-1348 Louvain-la-Neuve, Belgium

Коефицијенти брзине за дисоцијацију O_3^+ ударом електрона на фрагменте O^+ и O_2^+ израчунати су за нови, препоручени скуп података ефективних пресека и за различите услове судара. Коришћена су два скупа ефективних пресека, које су недавно измериле различите експерименталне групе. Ови пресеци се међусобно значајно разликују, али су ренормирани и оптимизовани за кохерентну базу података. Коефицијенти брзине за фрагментацију катјона озона су одређени коришћењем Максвелове и неравнотежне функције расподеле енергије електрона. У случају Максвелове дистрибуције, средње енергије електрона покривају опсег од нула до 2 keV. Неравнотежне функције расподеле енергије електрона су усвојене из недавних посматрања електрона у 3-D експерименту са плазмом изведеном на свемирском броду WIND. Неравнотежни коефицијенти брзине су процењени за средње енергије електрона од 4 до 80 eV. Наглашена је улога могућег доприноса дисоцијације O_3^+ електронским ударом у оштећењу озонског омотача.

(Примљено 9. новембра, ревидирано 11. децембра, прихваћено 13. децембра 2021)

REFERENCES

1. M. J. Molina, F. S. Rowland, *Nature* **249** (1974) 810 (https://doi.org/10.1038/249810a0)
2. J. C. Farman, B. G. Gardiner, J. D. Shanklin, *Nature* **315** (1985) 207 (https://doi.org/10.1038/315207a0)
3. V. Vaida, J. D. Simon, *Science* **268** (1995) 1443 (https://doi.org/10.1126/science.268.5216.1443)
4. J. A. Davies, W. M. Johnstone, N. J. Mason, P. Biggs, R. P. Wayne, *J. Phys., B* **26** (1993) L767 (https://doi.org/10.1088/0953-4075/26/21/008)

5. M. Allan, K. R. Asmis, D. B. Popović, M. Stepanović, N. J. Mason, J. A. Davies, *J. Phys., B* **29** (1996) 3487 (https://doi.org/10.1088/0953-4075/29/15/020)
6. C. J. Sweeney, T. W. Shyn, *Phys. Rev., A* **53** (1996) 1576 (https://doi.org/10.1103/PhysRevA.53.1576)
7. M. W. Siegel, *Int. J. Mass Spectrom. Ion Phys.* **44** (1982) 19 (https://doi.org/10.1016/0020-7381(82)80036-3)
8. K. A. Newson, S. M. Luc, S. D. Price, N. J. Mason, *Int. J. Mass Spectrom. Ion Process.* **148** (1995) 203 (https://doi.org/10.1016/0168-1176(95)04300-A)
9. Y.-K. Kim, W. Hwang, N. M. Weinberger, M. A. Ali, M. E. Rudd, *J. Chem. Physics* **106** (1997) 1026 (https://doi.org/10.1063/1.473186)
10. Y.-K. Kim, K. K. Irikura, M. E. Rudd, M. A. Ali, P. M. Stone, J. Chang, J. S. Coursey, R. A. Dragoset, A. R. Kishore, K. J. Olsen, A. M. Sansonetti, G. G. Wiersma, D. S. Zucker, M. A. Zucker, *NIST Standard Reference Database 107, Electron-Impact Cross Sections for Ionization and Excitation*, Vol. 107, 2005, p. 1, NIST, Gaithersburg (http://www.nist.gov/pml/data/ionization/index.cfm)
11. N. J. Mason, J. M. Gingell, J. A. Davies, H. Zhao, I. C. Walker, M. R. F. Siggel, *J. Phys., B* **29** (1996) 3075 (https://doi.org/10.1088/0953-4075/29/14/019)
12. G. de Petris, *Mass Spectrom. Rev.* **22** (2003) 251 (https://doi.org/10.1002/mas.10053)
13. V. Zhaunerchyk, W. D. Geppert, M. Larsson, R. D. Thomas, E. Bahati, M. E. Bannister, M. R. Fogle, C. R. Vane, F. Osterdahl, *Phys. Rev. Lett.* **98** (2007) 223201 (https://doi.org/10.1103/PhysRevLett.98.223201)
14. M. L. Vestal, G. H. Mauclaire, *J. Chem. Phys.* **67** (1977) 3767 (https://doi.org/10.1063/1.435317)
15. S. H. M. Deng, C. R. Vane, M. E. Bannister, M. Fogle, *Phys. Rev., A* **82** (2010) 062715 (https://doi.org/10.1103/PhysRevA.82.062715)
16. D. S. Belić, X. Urbain, P. Defrance, *Phys. Rev., A* **91** (2015) 012703 (https://doi.org/10.1103/PhysRevA.91.012703)
17. J. Lecointre, D. S. Belić, H. Cherkani-Hassani, J. J. Jureta, P. Defrance. *J. Phys., B* **39** (2006) 3275 (https://doi.org/10.1088/0953-4075/39/16/011)
18. D. S. Belić, X. Urbain, H Cherkani-Hassani, P Defrance, *Phys. Rev., A* **95** (2017) 052702 (https://doi.org/10.1103/PhysRevA.95.052702)
19. D. S. Belić, M. M. Ristić, H.Cherkani-Hassani, X. Urbain, P. Defrance, *Eur. Phys. J., D* **74** (2020) 100 (https://doi.org/10.1140/epjd/e2020-100623-1)
20. M. Ristić, G. B. Poparić, D. S. Belić, *Chem. Phys.* **331** (2007) 410 (https://doi.org/10.1016/j.chemphys.2006.11.012)
21. R. P. Lin, in *Proceedings of the CESRA Workshop*, 1996, Nouan le Fuzelier, France, Springer, Berlin, 1997, p. 93
22. P. T. Verronen, C. J. Rodger, M. A. Clilverd, S. Wang, *J. Geophys. Res.* **116** (2011) D07307 (https://doi.org/10.1029/2010JD014965)
23. M. E. Andersson, P.T. Verronen, C. J. Rodger, M. A. Clilverd, A. Seppälä, *Nature Commun.* **5** (2014) 5197 (https://doi.org/10.1038/ncomms6197).